IEEE Access
Multidisciplinary | Rapid Review | Open Access Journal

Received December 20, 2018, accepted January 22, 2019, date of publication January 31, 2019, date of current version February 20, 2019.

*Digital Object Identifier 10.1109/ACCESS.2019.2896594*

# Decentralized Control of Multi-Parallel Grid-Forming DGs in Islanded Microgrids for Enhanced Transient Performance

**XIN HUANG[1], (Student Member, IEEE), KEYOU WANG[1], (Member, IEEE), JIAN QIU[2], LIJUN HANG[2], (Member, IEEE), GUOJIE LI[1], (Senior Member, IEEE), AND XINGANG WANG[3]**

[1]Department of Electrical Engineering, Shanghai Jiao Tong University, Shanghai 200240, China
[2]Renewable Energy and Microgrid Technology Laboratory, Hangzhou Dianzi University, Hangzhou 310018, China
[3]Electric Power Research Institute, State Grid Shanghai Municipal Electric Power Company, Shanghai 200080, China

Corresponding author: Keyou Wang (wangkeyou@sjtu.edu.cn)

This work was supported in part by the NSFC under Grant 51877133 and Grant 51477098, and in part by the State Grid Technology Program under Grant 52094017000Z.

**ABSTRACT** This paper proposes a novel decentralized control strategy for multiparallel grid-forming distributed generations (DGs) in an islanded microgrid. Different from most existing droop-based hierarchical control methods, the proposed scheme imposes a fixed system frequency that is independent of the load conditions. Additionally, a proper point of common coupling (PCC) voltage amplitude maintaining and proportional power sharing can be simultaneously achieved when dealing with variations in the load and DGs plug in/off. The transient performance of the system, as well as the power supply reliability, can be improved, as no extra restoration control layer or communications between the inverters are needed. Furthermore, the power-sharing ratio among the DG units can be changed online without affecting the voltage regulation performance, which enhances the power management flexibility. The PCC voltage regulation and the power-sharing performance of the proposed control strategy are ensured via the Lyapunov method. Finally, the effectiveness and practicability of the proposed approach are verified through real-time simulations and hardware experimental tests.

**INDEX TERMS** Improved transient performance, islanded microgrid, multiparallel grid-forming DGs, PCC voltage regulation, proportional power sharing.

## I. INTRODUCTION

Microgrids have become an effective method for reliably integrating distributed generations (DGs) into power systems, and microgrids can also be operated more flexibly in both the grid connected mode and islanded mode [1], [2]. During the islanded operation, multiparallel connected inverter-interfaced DGs can act as grid-forming units to setup the point of common coupling (PCC) voltage and provide active and reactive power to the loads. It is crucial to achieve good PCC voltage regulation for system stability and load supply reliability. Besides, the load power should be shared by the DG units in proportion to their power ratings or available unused capacities [3], [4], which can avoid overstressing and delay aging of the sources.

The droop control method has been widely applied to grid-forming inverters to set up the PCC voltage and to achieve the proper power sharing among DG units in a decentralized manner [5]–[8]. Nevertheless, the major drawback of the droop control is the inherent trade-off between the voltage regulation and power sharing accuracy, i.e., a steeper droop can ensure better load sharing, yet it results in larger voltage deviations and more oscillatory transient response [9], [10]. Moreover, the deviations are load-dependent and cannot be avoided during the transients due to the droop mechanism.

To compensate the deviations in amplitude and frequency of the PCC voltage caused by the primary droop control and restore them to the normal value, an external control loop is commonly installed as the secondary control based on the hierarchical control framework [11]–[13]. However, this vertical hierarchical control mechanism can reduce the dynamics of the system and limit the speed of the voltage regulation, it could be unacceptable in applications where

The associate editor coordinating the review of this manuscript and approving it for publication was Salvatore Favuzza.

power quality is the main concern, and the reliable power supply may not be ensured during the transients.

Optimum load sharing is another important issue for grid-forming DGs [14], [15]. It is of great benefit if the load power can be flexibly shared by each grid-forming DG according to different operation requirements, such as proportional to the DGs' available unused capacities or considering the DGs' economic generation. However, in an islanded mode, it is hardly feasible to on-line adjust the load sharing ratio among the droop based grid-forming DGs, since an inappropriate change in droop coefficients may adversely affect the voltage quality and system stability.

Considering the above challenges, a novel decentralized control strategy is proposed for multiparallel grid-forming DGs in an islanded microgrid. The control law is designed based on the reformulated dynamic model of the system and developed using a filter tracking error method, which comes from some filtered error notions standard in nonlinear control theory [16], [17] with some interesting features, such as a high periodic tracking performance and being easily compatible with the robust control method. The system stability and power sharing capability are theoretically proven under different operating conditions (e.g., normal operation and DG fault outage). The salient features of the proposed control technique are as follows:

1) When dealing with the microgrid contingency event, e.g., large or rapid load variation and the DG fault condition, the proposed control strategy can eliminate the trade-off between superior voltage regulation and power sharing accuracy within a single control layer. Thus, enhanced transient performance can be achieved;
2) The arbitrary power sharing ratio and flexible power sharing performance among the DG units can be achieved without affecting the voltage regulation performance;
3) There is no central controller and intercommunication between DG units, which improves the system stability and allows for robust plug-and-play operation.

The remainder of this paper is organized as follows. Section II discusses the limitations of the existing droop-based hierarchical control structure for an islanded microgrid, then a novel decentralized controller-based microgrid structure is introduced for enhanced transient performance. The design of the proposed decentralized control law is shown in Section III. A theoretical analysis on voltage regulation and power sharing performance of the proposed controller is presented in Section IV. The effectiveness and practicability of the proposed method are verified through real-time simulations and hardware experimental tests in Section V. Meanwhile, the novelty of the proposed method is highlighted by comparing the existing droop control methodologies. Section VI summarizes the paper.

## II. DISCUSSION OF CONTROL STRUCTURES

In this work, it is considered that the multiparallel grid-forming DG units are installed in a common switching station, as shown in Fig. 1. Therefore, these DG units are considered to be connected to a common AC bus via the line impedances, whereas the grid impedance between each DG connection point is negligible. The main task of this switching station is to keep the PCC voltage stable. In the meantime, the aggregated current ($i_{total}$) supplied to the local load or injected into the remainder of the microgrid should be properly shared among grid-forming DG units according to their ratings. However, for a modern microgrid, the control objectives are becoming various and ambitions, such as a robust plug-and-play operation, a higher reliable power supply with superior transient performance, as well as maximal accuracy and flexibility in load power sharing [9].

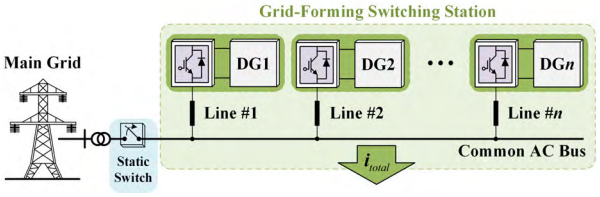


**FIGURE 1.** Diagram of a common switching station with *n* parallel grid-forming DGs for an islanded micro-grid.

It is a significant challenge for most of the existing droop-based control methods due to the limitation of its control structure: inner voltage/current control, primary control and secondary control in a vertical hierarchy, as shown in Fig. 2(a). Since each layer may interact in an adverse way

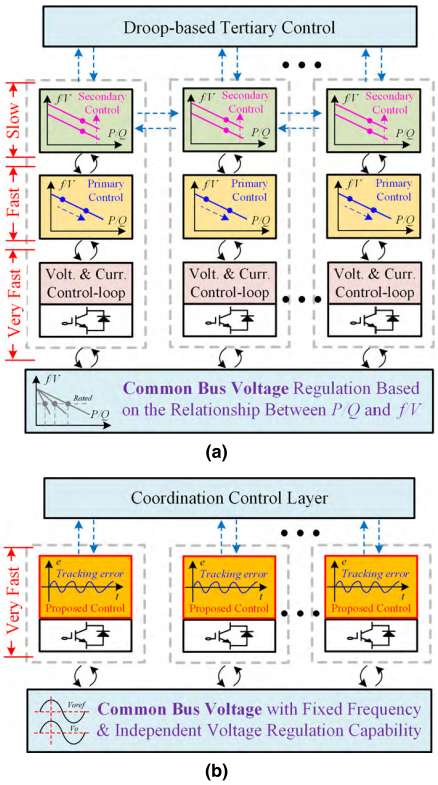


**FIGURE 2.** Control structure comparison. (a) Droop control-based hierarchy. (b) Proposed decentralized control-based hierarchy.

unless a time-scale separation is enforced, when an unexpected load change or DG fault outage occurs, the aforementioned two control objectives, maintaining the PCC voltage at the rated value and proportionally sharing the load power, must be realized by the coordination of three control layers, which significantly limits the response speed of the system, while the power supply reliability, especially for the sensitive load, will not be ensured.

Different from the droop control mechanism, the proposed control law is developed based on the filtered tracking error control method as mentioned above. Accordingly, this control strategy imposes a fixed system frequency independent of the loading conditions, so the proper maintenance of the voltage amplitude and proportional load power sharing can be guaranteed at the same time during and after the transients (e.g., load variation, DGs plug in/off). As a result, no extra restoration/compensation control layer is needed in this control structure (see Fig. 2(b)), the potentials of inverter-interfaced DGs in terms of response speed and flexibility can be fully unleashed, and the microgrid system dynamics and transient performance can be significantly improved. Notably, the coordination control layer is reserved here to deal with economic dispatch, operation scheduling, and power management issues. The corresponding control schemes and its implementation is not the focus of this paper.

## III. PROPOSED DECENTRALIZED CONTROL SCHEME

### A. SYSTEM MODELLING

According to the schematic model of the investigated system shown in Fig. 3, each DG unit is assumed to be three-phase symmetrical. Thus, the dynamic model of the *ith* DG can be obtained in a stationary reference frame as follows:

*The LC filter circuit:*

$$L_{fi}\begin{bmatrix}\dot{i}_{\alpha i}\\ \dot{i}_{\beta i}\end{bmatrix} = -R_{fi}\begin{bmatrix}i_{\alpha i}\\ i_{\beta i}\end{bmatrix} + \begin{bmatrix}v_{\alpha i}\\ v_{\beta i}\end{bmatrix} - \begin{bmatrix}v_{c\alpha i}\\ v_{c\beta i}\end{bmatrix} \tag{1}$$

*The line impedance circuit:*

$$\begin{bmatrix}v_{c\alpha i}\\ v_{c\beta i}\end{bmatrix} = \begin{bmatrix}v_{o\alpha}\\ v_{o\beta}\end{bmatrix} + L_{li}\begin{bmatrix}\dot{i}_{o\alpha i}\\ \dot{i}_{o\beta i}\end{bmatrix} + R_{li}\begin{bmatrix}i_{o\alpha i}\\ i_{o\beta i}\end{bmatrix} \tag{2}$$

where the subscript $i$ refers to the index of the DG unit. $L_f$, $R_f$ and $C_f$ are the filter inductance, resistance and capacitor, respectively; $L_l$ and $R_l$ represent the equivalent line inductance and resistance between the DG and the common bus, respectively. In the stationary reference frame, variables $i_\alpha$, $i_\beta$ and $v_\alpha$, $v_\beta$ are the inverter output current and the control input of the inverter, respectively; $v_{c\alpha}$, $v_{c\beta}$ and $v_{o\alpha}$, $v_{o\beta}$ are the voltage across the filter capacitor and the PCC voltage, respectively; $i_{o\alpha}$ and $i_{o\beta}$ are the current feeding into the AC bus.

Considering a general system composed of $n$ grid-forming DGs connected in parallel, the aggregated current feeding into the AC bus from the entire grid-forming units is represented as $i_{total}$ and satisfies $i_{total} = \sum_{i=1}^{n} i_{oi}$. We define a positive constant $\lambda_i$ that satisfies $\sum_{i=1}^{n} \lambda_i = 1$, then the grid feeding current of each DG unit can be represented as

$$\begin{cases} i_{o\alpha i} = \lambda_i \cdot i_{total\alpha} \\ i_{o\beta i} = \lambda_i \cdot i_{total\beta} \end{cases} \tag{3}$$

Thus, (2) can be rewritten as

$$\begin{bmatrix}v_{c\alpha i}\\ v_{c\beta i}\end{bmatrix} = \begin{bmatrix}v_{o\alpha}\\ v_{o\beta}\end{bmatrix} + L_{li}\lambda_i\begin{bmatrix}\dot{i}_{total\alpha}\\ \dot{i}_{total\beta}\end{bmatrix} + R_{li}\lambda_i\begin{bmatrix}i_{total\alpha}\\ i_{total\beta}\end{bmatrix} \tag{4}$$

Further, the dynamics of the capacitor can be utilized to derive the relationship between these two circuit loops as

$$C_{fi}\begin{bmatrix}\dot{v}_{c\alpha i}\\ \dot{v}_{c\beta i}\end{bmatrix} = \begin{bmatrix}i_{\alpha i}\\ i_{\beta i}\end{bmatrix} - \begin{bmatrix}i_{o\alpha i}\\ i_{o\beta i}\end{bmatrix} = \begin{bmatrix}i_{\alpha i}\\ i_{\beta i}\end{bmatrix} - \lambda_i\begin{bmatrix}i_{total\alpha}\\ i_{total\beta}\end{bmatrix} \tag{5}$$

Since the above $n$ DG units serve a common AC bus, (5) can be expressed as

$$\begin{bmatrix}\sum_{i=1}^{n} C_{fi}\dot{v}_{c\alpha i}\\ \sum_{i=1}^{n} C_{fi}\dot{v}_{c\beta i}\end{bmatrix} = \begin{bmatrix}\sum_{i=1}^{n} i_{\alpha i}\\ \sum_{i=1}^{n} i_{\beta i}\end{bmatrix} - \begin{bmatrix}i_{total\alpha}\\ i_{total\beta}\end{bmatrix} \tag{6}$$

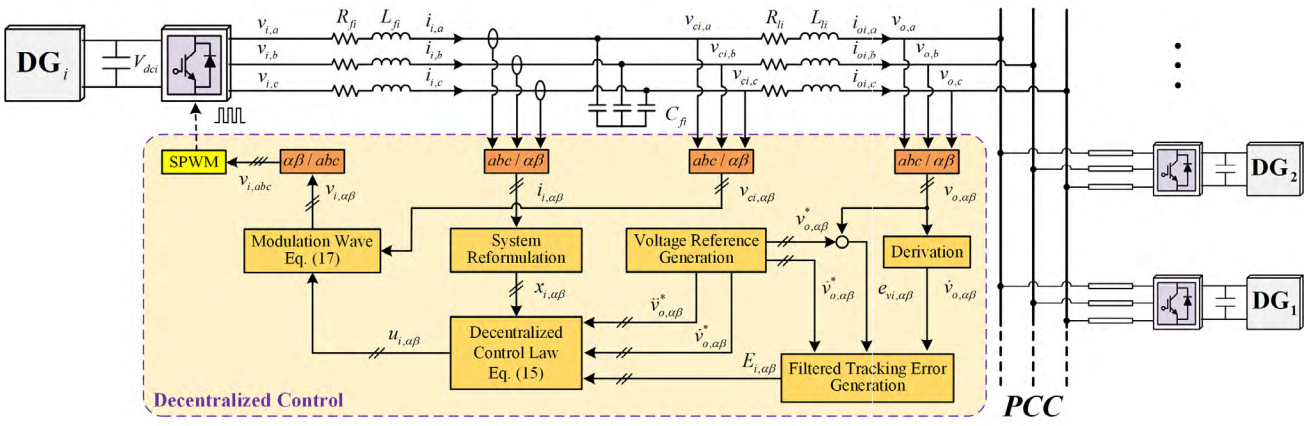


**FIGURE 3.** Diagram of the proposed control strategy for parallel connected grid-forming DGs in an islanded microgrid.

Submitting the time derivative of (4) into (6) yields

$$\begin{bmatrix} \sum_{i=1}^{n} C_{fi}\dot{v}_{o\alpha} \\ \sum_{i=1}^{n} C_{fi}\dot{v}_{o\beta} \end{bmatrix} = \begin{bmatrix} \sum_{i=1}^{n} i_{\alpha i} \\ \sum_{i=1}^{n} i_{\beta i} \end{bmatrix} - \begin{bmatrix} i_{total\alpha} + \sum_{i=1}^{n} C_{fi}\lambda_i \left(R_{li}\dot{i}_{total\alpha} + L_{li}\ddot{i}_{total\alpha}\right) \\ i_{total\beta} + \sum_{i=1}^{n} C_{fi}\lambda_i \left(R_{li}\dot{i}_{total\beta} + L_{li}\ddot{i}_{total\beta}\right) \end{bmatrix} \tag{7}$$

According to (7) and (1), the dynamic model of the system can be reformulated as

$$\begin{aligned} \dot{\boldsymbol{v}}_o &= \sum_{i=1}^{n} \boldsymbol{x}_i - \boldsymbol{d} \\ \dot{\boldsymbol{x}}_i &= \boldsymbol{u}_i \end{aligned} \tag{8}$$

where $\boldsymbol{v}_o = \left[v_{o\alpha} v_{o\beta}\right]^T$, $\boldsymbol{x}_i = \left[x_{\alpha i} x_{\beta i}\right]^T = \left[\frac{i_{\alpha i}}{C_f} \frac{i_{\beta i}}{C_f}\right]^T$ with $C_f = \sum_{i=1}^{n} C_{fi}$. $\boldsymbol{u}_i$ is considered as an intermediate variable related to the control input, $\boldsymbol{d}$ is regarded as the unknown disturbance item, which can be represented as

$$\boldsymbol{u}_i = \frac{1}{L_{fi}C_f}\left(\boldsymbol{v}_i - R_{fi}\boldsymbol{i}_i - \boldsymbol{v}_{ci}\right) \tag{9}$$

$$\boldsymbol{d} = \frac{1}{C_f}\left[\boldsymbol{i}_{total} + \sum_{i=1}^{n} C_{fi}\lambda_i \left(R_{li}\dot{\boldsymbol{i}}_{total} + L_{li}\ddot{\boldsymbol{i}}_{total}\right)\right] \tag{10}$$

where $\boldsymbol{u}_i = \left[u_{\alpha i} u_{\beta i}\right]^T$, $\boldsymbol{d} = \left[d_\alpha d_\beta\right]^T$, and $\boldsymbol{v}_i = \left[v_{\alpha i} v_{\beta i}\right]^T$, $\boldsymbol{i}_i = \left[i_{\alpha i} i_{\beta i}\right]^T$, $\boldsymbol{v}_{ci} = \left[v_{c\alpha i} v_{c\beta i}\right]^T$, $\boldsymbol{i}_{total} = \left[i_{total\alpha} i_{total\beta}\right]^T$.

It can be seen from (9) that the input transformation from $\boldsymbol{v}_i$ to $\boldsymbol{u}_i$ is invertible, which demonstrates that the final voltage command of each inverter can be produced by the proper design of $\boldsymbol{u}_i$.

### B. PROPOSED DECENTRALIZED CONTROL LAW

Based on the reformulated system model expressed in (8), the decentralized controller is developed by using a filtered tracking error-based method, which helps to maneuver the output bus voltage components in stationary frame to track their desired trajectories $v_{o\alpha}^*$ and $v_{o\beta}^*$ via their respective control laws. The desired $\alpha$, $\beta$ axis output trajectories can be generated as $v_{o\alpha}^* = V\sin(\omega t)$ and $v_{o\beta}^* = V\sin(\omega t - \pi/2)$, respectively, where $V$ is the amplitude of the phase-voltage, and $\omega$ is the system's angular frequency.

The tracking error is introduced as $\boldsymbol{e}_v = \boldsymbol{v}_o - \boldsymbol{v}_o^*$, and the filtered tracking errors can be defined as $\boldsymbol{E} = q\boldsymbol{e}_v + \dot{\boldsymbol{e}}_v$, $\boldsymbol{r} = \mu\boldsymbol{E} + \dot{\boldsymbol{E}}$ with $\boldsymbol{v}_o^* = \left[v_{o\alpha}^* v_{o\beta}^*\right]^T$, $\boldsymbol{e}_v = \left[e_{v\alpha} e_{v\beta}\right]^T$, $\boldsymbol{E} = \left[E_\alpha E_\beta\right]^T$ and $\boldsymbol{r} = \left[r_\alpha r_\beta\right]^T$, $q$ and $\mu$ are positive constants.

Recalling the system dynamics in (8) and taking the first and second derivative of $\boldsymbol{E}$ yields

$$\begin{aligned} \dot{\boldsymbol{E}} &= q\dot{\boldsymbol{v}}_o + \ddot{\boldsymbol{v}}_o - q\dot{\boldsymbol{v}}_o^* - \ddot{\boldsymbol{v}}_o^* \\ &= q\sum_{i=1}^{n} \boldsymbol{x}_i + \sum_{i=1}^{n} \boldsymbol{u}_i - q\boldsymbol{d} - \dot{\boldsymbol{d}} - q\dot{\boldsymbol{v}}_o^* - \ddot{\boldsymbol{v}}_o^* \end{aligned} \tag{11}$$

$$\begin{aligned} \ddot{\boldsymbol{E}} &= q\ddot{\boldsymbol{v}}_o + \boldsymbol{v}_o - q\ddot{\boldsymbol{v}}_o^* - \boldsymbol{v}_o^* \\ &= q\sum_{i=1}^{n} \dot{\boldsymbol{x}}_i + \sum_{i=1}^{n} \dot{\boldsymbol{u}}_i - q\dot{\boldsymbol{d}} - \ddot{\boldsymbol{d}} - q\ddot{\boldsymbol{v}}_o^* - \boldsymbol{v}_o^* \end{aligned} \tag{12}$$

A Lyapunov function is defined to develop the tracking controller as

$$V = \frac{1}{2}\boldsymbol{E}^T\boldsymbol{E} + \frac{1}{2}\rho\boldsymbol{r}^T\boldsymbol{r} \tag{13}$$

where $\rho = \frac{1}{\mu^2}$. Differentiating (13) with respect to time and considering (11)-(12) we can obtain

$$\begin{aligned} \dot{V} &= \boldsymbol{E}^T\dot{\boldsymbol{E}} + \rho\boldsymbol{r}^T\dot{\boldsymbol{r}} \\ &= \boldsymbol{E}^T\left(\boldsymbol{r} - \mu\boldsymbol{E}\right) + \rho\boldsymbol{r}^T\left(\mu\dot{\boldsymbol{E}} + \ddot{\boldsymbol{E}}\right) \\ &= -\mu\left\|\boldsymbol{E}\right\|^2 + \rho\boldsymbol{r}^T\left\{\frac{\boldsymbol{E}}{\rho} + \mu\dot{\boldsymbol{E}} + q\sum_{i=1}^{n}\dot{\boldsymbol{x}}_i \right. \\ &\quad \left. + \sum_{i=1}^{n}\dot{\boldsymbol{u}}_i - q\dot{\boldsymbol{d}} - \ddot{\boldsymbol{d}} - q\ddot{\boldsymbol{v}}_o^* - \boldsymbol{v}_o^*\right\} \end{aligned} \tag{14}$$

According to the Lyapunov stability theory, the control law should be properly designed to ensure $\dot{V} < 0$. Thus, solving for the control law of the *ith* DG yields

$$\begin{aligned} \boldsymbol{u}_i = &-q\boldsymbol{x}_i - m_i\cdot\left[\left(\mu + k_r\right)\boldsymbol{E} - q\dot{\boldsymbol{v}}_o^* - \ddot{\boldsymbol{v}}_o^*\right] \\ &- m_i\cdot\int_0^t\left(\mu k_r + \frac{1}{\rho}\right)\boldsymbol{E}(\tau)\cdot d\tau \end{aligned} \tag{15}$$

where $k_r$ is a positive constant, and $m_i$ is defined as a weight coefficient with $0 < m_i < 1$. Taking the derivate of $\boldsymbol{u}_i$ with respect to time yields

$$\begin{aligned} \dot{\boldsymbol{u}}_i &= -q\dot{\boldsymbol{x}}_i - m_i\cdot\left[\left(\mu + k_r\right)\dot{\boldsymbol{E}} - q\ddot{\boldsymbol{v}}_o^* - \boldsymbol{v}_o^*\right] \\ &\quad - m_i\cdot\left(\mu k_r + \frac{1}{\rho}\right)\boldsymbol{E} \\ &= -q\dot{\boldsymbol{x}}_i - m_i\cdot\left(\mu\dot{\boldsymbol{E}} + k_r\boldsymbol{r} - q\ddot{\boldsymbol{v}}_o^* - \boldsymbol{v}_o^* + \frac{\boldsymbol{E}}{\rho}\right) \end{aligned} \tag{16}$$

The control law ensures that under specific conditions $\dot{V} < 0$, so that the stability of the proposed controller can be guaranteed. The detailed proof can be found in Section IV.

Finally, the control law $\boldsymbol{u}_i$ can be used to generate the reference wave $\boldsymbol{v}_i$ for the pulse width modulation (PWM) control of *ith* inverter as follows

$$\boldsymbol{v}_i = R_{fi}\boldsymbol{i}_i + L_{fi}C_f\boldsymbol{u}_i + \boldsymbol{v}_{ci} \tag{17}$$

The implementation of the control strategy is shown in Fig. 3. Notice that the decentralized controller has no central control board and every module uses its own individual control law mostly based on its local information, such as output current, capacitance voltage as well as the preset

references curves $\boldsymbol{v}_o^*$, $\dot{\boldsymbol{v}}_o^*$, and $\ddot{\boldsymbol{v}}_o^*$ and the weight coefficient $m_i$ for the individual DG inverter. Since the distance between DG units and the common bus is in a medium or small microgrid scale, the bus voltage feedback signals can also be acquired in a decentralized manner. Moreover, no inter communication is needed between different DG units. As a result, the system's redundancy and reliability can be improved.

## IV. PCC VOLTAGE REGULATION AND POWER SHARING PERFORMANCE

In this section, the PCC voltage regulation and power sharing capability of the proposed control are theoretically analyzed. Additionally, the system performance in the case of DG outage is evaluated accordingly.

### A. PCC VOLTAGE REGULATION PERFORMANCE

First, the system stability and voltage tracking performance of the proposed controller under a normal operation is evaluated. It can be illustrated that for the investigated system, the following characteristics can be held under the proposed decentralized control law:

1) Superior references tracking performance can be ensured for the PCC voltage $\boldsymbol{v}_o$ with a fast transient response and small tracking errors;
2) The global stability of the closed-loop system is guaranteed along with all signals bounded.

To aid the proof of the system stability, the following reasonable assumption is introduced before proceeding.

*Assumption:* The aggregated feeding current $\boldsymbol{i}_{total}$, and a finite number of its time derivatives are bounded [18]–[20]. Therefore, $\boldsymbol{d}$ along with its respective first and second time derivatives, are unknown but bounded, that is

$$\begin{cases} |d_\alpha| \le D_{0,\alpha}; & |\dot{d}_\alpha| \le D_{1,\alpha}; & |\ddot{d}_\alpha| \le D_{2,\alpha} \\ |d_\beta| \le D_{0,\beta}; & |\dot{d}_\beta| \le D_{1,\beta}; & |\ddot{d}_\beta| \le D_{2,\beta} \end{cases} \tag{18}$$

where $D_{0,\alpha}$, $D_{1,\alpha}$, $D_{2,\alpha}$ and $D_{0,\beta}$, $D_{1,\beta}$, $D_{2,\beta}$ are unknown positive constants. It should be noted that the values of these boundary limits are not required in the implementation of the proposed control method.

Recalling (16) and considering the sum of $\dot{\boldsymbol{u}}_i$ ($i = 1, 2, \ldots, n$) we have

$$\sum_{i=1}^{n} \dot{\boldsymbol{u}}_i = -q \sum_{i=1}^{n} \dot{\boldsymbol{x}}_i - m \cdot \left( \mu \dot{\boldsymbol{E}} + k_r \boldsymbol{r} - q \ddot{\boldsymbol{v}}_o^* - \boldsymbol{v}_o^* + \frac{\boldsymbol{E}}{\rho} \right) \tag{19}$$

where the weight coefficient $m = \sum_{i=1}^{n} m_i$. Submitting (19) into (14) yields

$$\dot{V} = -\mu \|\boldsymbol{E}\|^2 - c \cdot \rho \|\boldsymbol{r}\|^2 - \rho \boldsymbol{r}^T \left( \boldsymbol{V}_r + q\dot{\boldsymbol{d}} + \ddot{\boldsymbol{d}} \right) \tag{20}$$

where

$$\begin{cases} c = m k_r - (1 - m)\, \mu \\ \boldsymbol{V}_r = (1 - m) \cdot \left( q \ddot{\boldsymbol{v}}_o^* + \boldsymbol{v}_o^* \right) \end{cases} \tag{21}$$

Since $m = \sum_{i=1}^{n} m_i = 1$ is required in the normal operation, the derivative of the Lyapunov function can be developed as

$$\begin{aligned} \dot{V} &= -\mu \|\boldsymbol{E}\|^2 - \rho k_r \|\boldsymbol{r}\|^2 - \rho \boldsymbol{r}^T (q\dot{\boldsymbol{d}} + \ddot{\boldsymbol{d}}) \\ &\le -\mu \|\boldsymbol{E}\|^2 - \rho k_r \|\boldsymbol{r}\|^2 \\ &\quad + \rho |r_\alpha| \left( q |\dot{d}_\alpha| + |\ddot{d}_\alpha| \right) + \rho |r_\beta| \left( q |\dot{d}_\beta| + |\ddot{d}_\beta| \right) \end{aligned} \tag{22}$$

Recalling the Assumption and choosing $0 < \varepsilon < 2k_r$ yields

$$\begin{aligned} \dot{V} &\le -\mu \|\boldsymbol{E}\|^2 - \rho k_r \|\boldsymbol{r}\|^2 \\ &\quad + \rho |r_\alpha| (q D_{1,\alpha} + D_{2,\alpha}) + \rho |r_\beta| (q D_{1,\beta} + D_{2,\beta}) \\ &\le -\mu \|\boldsymbol{E}\|^2 - \rho k_r \|\boldsymbol{r}\|^2 + \rho \frac{\varepsilon}{2} \|\boldsymbol{r}\|^2 \\ &\quad + \rho \frac{1}{2\varepsilon} (q D_{1,\alpha} + D_{2,\alpha})^2 + \rho \frac{1}{2\varepsilon} (q D_{1,\beta} + D_{2,\beta})^2 \\ &\le -2\sigma V + \eta \end{aligned} \tag{23}$$

where

$$\begin{cases} \sigma = \min \left\{ \mu, k_r - \dfrac{\varepsilon}{2} \right\} \\ \eta = \rho \dfrac{1}{2\varepsilon} \left[ \left( q D_{1,\alpha} + D_{2,\alpha} \right)^2 + \left( q D_{1,\beta} + D_{2,\beta} \right)^2 \right] \end{cases} \tag{24}$$

According to [17, Lemma 1.2], one has that

$$\lim_{t \to \infty} \|\boldsymbol{E}\| \le \sqrt{\frac{\eta}{\sigma}}; \quad \lim_{t \to \infty} \|\boldsymbol{r}\| \le \sqrt{\frac{\eta}{\sigma \rho}} \tag{25}$$

It can be obtained from (25) that the filtered tracking error $\boldsymbol{E}$ and $\boldsymbol{r}$ are bounded. Moreover, according to the definition of $\sigma$ and $\eta$ in (24), in order to meet the practical operation requirement the tracking error can be rendered arbitrarily small by properly setting the user-defined constants $\mu$, $q$ and $k_r$. Thus, the first assertion can be held.

Since $\boldsymbol{e}_v$ and $\dot{\boldsymbol{e}}_v$ are the outputs of a stable linear system with input $\boldsymbol{E}$, which is proven to be bounded in (25), $\boldsymbol{e}_v$ and $\dot{\boldsymbol{e}}_v$ are also bounded. Similarly, since $\dot{\boldsymbol{E}} = \boldsymbol{r} - \mu \boldsymbol{E}$ is bounded, then $\ddot{\boldsymbol{e}}_v = q\dot{\boldsymbol{e}}_v - \dot{\boldsymbol{E}}$ is bounded as well. Because $\boldsymbol{v}_o^*$, $\dot{\boldsymbol{v}}_o^*$, and $\ddot{\boldsymbol{v}}_o^*$ are all bounded, the output bus voltage $\boldsymbol{v}_o$ together with $\dot{\boldsymbol{v}}_o$ and $\ddot{\boldsymbol{v}}_o$ are also bounded. With the assumption and application of (7), it can be inferred that $\sum_{i=1}^{n} \boldsymbol{x}_i = \dot{\boldsymbol{v}}_o + \boldsymbol{d}$ and $\sum_{i=1}^{n} \boldsymbol{u}_i = \ddot{\boldsymbol{v}}_o + \dot{\boldsymbol{d}}$ are bounded. Hence, standard linear analysis methods can be applied to prove that $\boldsymbol{x}_i$ are bounded for $i \in \{1, 2, \ldots, n\}$. Moreover, the definition of $\boldsymbol{x}_i = \boldsymbol{i}_i / C_f$ gives $\boldsymbol{i}_i = C_f \boldsymbol{x}_i$. Thus, $\boldsymbol{i}_i$ are bounded, and the second assertion holds.

However, in the case of one or more DGs fault outage, since the condition that $m = \sum_{i=1}^{n} m_i = 1$ cannot be satisfied, the features from (22) to (25) should be rederived for evaluating the voltage regulation performance. Recalling $\dot{V}$ expressed in (20)-(21) and considering the actual meaning of $m$, $c > 0$ can be commonly ensured in most cases by choosing the appropriate parameters $k_r$ and $\mu$. Since $\ddot{\boldsymbol{v}}_o^*$ and $\boldsymbol{v}_o^*$ are predefined reference trajectories, $\boldsymbol{V}_r$ is apparently bounded, so that it can be processed in a similar way with $\boldsymbol{d}$ in (18). Thus, the first and second assertions of the PCC voltage regulation can still be held.

Moreover, consider the remaining item $\boldsymbol{V}_r$ in (21) after the DG outage, it can be inferred that $\eta$ depicted in (23)-(25) will become larger if one or more DGs are out of service,

which may lead to an increase in the voltage tracking error according to (25). A practical way to eliminate the additional error is to update the weight coefficients $m_i$ through the coordination control layer. Once the weight coefficients are properly reassigned, the amplitude of the PCC voltage can be restored to its original value in the normal operation. In addition, since this coordination control is only responsible for steady-state performance regulation, only an unidirectional low bandwidth communication link needs to be employed for sending the weight coefficients in certain intervals, and the requirement of the communication is low compared to the droop-based secondary controller, which constantly transmits control signals [21].

### B. ANALYSIS OF POWER SHARING PERFORMANCE

To represent the effectiveness of the proportional current sharing between any two operating DGs connected in parallel, e.g., $DG_i$ and $DG_j$, the current sharing error is defined as

$$i_{error}^{(i,j)} = \left| \frac{i_{oi}}{m_i} - \frac{i_{oj}}{m_j} \right| \tag{26}$$

where $m_i$ and $m_j$ are the weight coefficients of these two DG units, respectively. According to the system dynamics depicted in (7) and the proposed control law, the following fact holds: The weight coefficient of any two $DG_i$ and $DG_j$ is set as $(m_i : m_j)$, which leads the current sharing error defined in (26) to be exponentially close to zero as time goes to infinity.

Considering the following Lyapunov function

$$V_c = \frac{1}{2} \sum_{i=1}^{n} \sum_{j=1, j\neq i}^{n} \left( \frac{\boldsymbol{x}_i}{m_i} - \frac{\boldsymbol{x}_j}{m_j} \right)^T \cdot \left( \frac{\boldsymbol{x}_i}{m_i} - \frac{\boldsymbol{x}_j}{m_j} \right) \tag{27}$$

Recalling the second equation in (7) and the control law in (15), the derivative of $V_c$ can be expressed as

$$\begin{aligned}
\dot{V}_c &= \sum_{i=1}^{n} \sum_{j=1, j\neq i}^{n} \left( \frac{\boldsymbol{x}_i}{m_i} - \frac{\boldsymbol{x}_j}{m_j} \right)^T \left( \frac{\boldsymbol{u}_i}{m_i} - \frac{\boldsymbol{u}_j}{m_j} \right) \\
&= \sum_{i=1}^{n} \sum_{j=1, j\neq i}^{n} \left( \frac{\boldsymbol{x}_i}{m_i} - \frac{\boldsymbol{x}_j}{m_j} \right)^T \left\{ -q \frac{\boldsymbol{x}_i}{m_i} + q \frac{\boldsymbol{x}_j}{m_j} \right. \\
&\quad - \left[ (\mu + k_r) \boldsymbol{E} - q \dot{\boldsymbol{v}}_o^* - \ddot{\boldsymbol{v}}_o^* - \int_0^t \left( \mu k_r + \frac{1}{\rho} \right) \boldsymbol{E}(\tau) d\tau \right] \\
&\quad \left. + \left[ (\mu + k_r) \boldsymbol{E} - q \dot{\boldsymbol{v}}_o^* - \ddot{\boldsymbol{v}}_o^* - \int_0^t \left( \mu k_r + \frac{1}{\rho} \right) \boldsymbol{E}(\tau) d\tau \right] \right\} \\
&= -\sum_{i=1}^{n} \sum_{j=1, j\neq i}^{n} q \left( \frac{\boldsymbol{x}_i}{m_i} - \frac{\boldsymbol{x}_j}{m_j} \right)^T \left( \frac{\boldsymbol{x}_i}{m_i} - \frac{\boldsymbol{x}_j}{m_j} \right) \\
&= -2qV_c
\end{aligned} \tag{28}$$

By resorting to the standard Lyapunov synthesis [17], we have

$$\left| \frac{\boldsymbol{x}_i(t)}{m_i} - \frac{\boldsymbol{x}_j(t)}{m_j} \right| \leq \left| \frac{\boldsymbol{x}_i(0)}{m_i} - \frac{\boldsymbol{x}_j(0)}{m_j} \right| \cdot e^{-2qt} \tag{29}$$

for any $i, j = 1, 2, \ldots n$, $i \neq j$, where $\boldsymbol{x}_i(0)$ and $\boldsymbol{x}_j(0)$ are the initial values of $\boldsymbol{x}_i(t)$ and $\boldsymbol{x}_j(t)$, respectively.

Since $\boldsymbol{x}_i = \boldsymbol{i}_i / C_f$ and $\boldsymbol{x}_j = \boldsymbol{i}_j / C_f$, it can be concluded that the inverter output currents along with their respective weight coefficients will coverage to zero exponentially as time goes to infinity, i.e.,

$$\left| \frac{\boldsymbol{i}_i(t)}{m_i} - \frac{\boldsymbol{i}_j(t)}{m_j} \right| \leq \left| \frac{\boldsymbol{i}_i(0)}{m_i} - \frac{\boldsymbol{i}_j(0)}{m_j} \right| \cdot e^{-2qt} \tag{30}$$

for $\forall i, j \in \{1, 2, \ldots, n\}\, i \neq j$, where $\boldsymbol{i}_i(0)$ and $\boldsymbol{i}_j(0)$ are the initial output current of $DG_i$ and $DG_j$, respectively.

It is worth noting that the final current feeding into the common bus from the inverter is slightly different from the inverter output current due to the reactive current flowing across the capacitor. Accordingly, the active current injected into the bus can still be shared accurately under different line impedances. Since the current on the capacitance can be somewhat affected due to the mismatched line impedance, the reactive power sharing accuracy can be degraded. On the other hand, since the PCC voltage tracking performance is well ensured, the total reactive load power can be well covered by each DG unit with a fast transient response. Based on these, the proposed control method can accommodate complex line impedances without explicitly accounting for their differences.

Furthermore, since the power sharing performance is independent of the sum of $m_i$, as well as the tracking error, according to the above analysis, $\|\boldsymbol{E}\|$ can be held for any DG unit, and the power sharing error for any two DG units can still be exponentially close to zero as time approaches infinity in the case of DG outage.

With the aforementioned characteristics, by properly setting the weight coefficient $m_i$ for the DG's controller, the injected power from different DG units can be flexibly dispatched. Additionally, no system retuning is needed since it has no adverse impact on the PCC voltage regulation. The implementation schemes can be realized and combined with the coordination control layer in different routes, such as a regular central controller to dispatch the weight coefficients to each DG unit with a proper interval of time for optimizing power management, or distributed algorithm, e.g., consensus methods, can be used for each inverter to calculate the weight coefficients.

## V. REAL-TIME SIMULATION AND EXPERIMENTAL TESTS

### A. REAL-TIME SIMULATION TESTS

The proposed control strategy is first tested and compared with the droop-based hierarchical control (DHC) approach [22] through the NI-PXI-based real-time simulation platform. According to the system configuration shown in Fig. 1, an islanded microgrid with four parallel-connected DG units and loads is developed in an electromagnetic transient simulation software Starsim [23], which directly links the investigated system model to an FPGA board, where the minimum step size for the inverter model running on the FPGA board is 1 us. The proposed control algorithm

is written by the LabVIEW software and deployed to the CPU, which acts as the controller. The two boards are both inside the PXI chassis and interact with one another through FIFO. The on-line programming and the operation results observation can be performed on a host machine, which communicates with the PXI chassis through a network.

The microgrid system and the control parameters are shown in Table 1. The cases study involves three scenarios: Scenario 1, Scenario 2, and Scenario 3, which correspond to a large load variation, DG unscheduled outage and power sharing ratio adjustment on-line, respectively. The scenario tests are activated in turn at different time points as described in the following.

**TABLE 1. Parameters of the real-time simulation tests.**

| *Items* | *Values*( $DG_1, DG_2, DG_3, DG_4$ ) | | | |
|---|---|---|---|---|
| ***Microgrid System Parameters*** | | | | |
| DC link voltage $V_{dc}$ (V) | 750 | | | |
| AC bus phase-voltage $V_{rms}$ (V) | 220 | | | |
| Fund frequency $f$ (Hz) | 50 | | | |
| Carrier frequency $f_c$ (kHz) | 20 | | | |
| Filter inductance $L_f$ (mH) | 1.6 | 1.8 | 2.0 | 2.2 |
| Filter capacitance $C_f$ ( $\mu F$ ) | 25 | 22 | 23 | 24 |
| Filter resistance $R_f$ ( $\Omega$ ) | 0.1 | 0.15 | 0.2 | 0.25 |
| Line resistance $R_l$ ( $\Omega$ ) | 0.5 | 0.3 | 0.2 | 0.3 |
| Line inductance $L_l$ (mH) | 0.2 | 0.25 | 0.3 | 0.25 |
| ***Proposed Controller Parameters*** | | | | |
| ( $q$ , $\mu$ , $k_r$ ) | (8000, 3500, 1500) | | | |
| Initial weight coefficient ( $m_i$ ) | 0.4 | 0.3 | 0.2 | 0.1 |
| ***Droop Controller Parameters*** | | | | |
| Voltage-loop PI controller ( $k_{pv}$,$k_{iv}$ ) | (0.1, 100) | | | |
| Current-loop PI controller ( $k_{pc}$,$k_{ic}$ ) | (0.2, 1) | | | |
| $P$-$\omega$ droop coefficient ( $n_{pi}\times10^3$ ) | 0.785 | 1.047 | 1.571 | 3.142 |
| $Q$-$V$ droop coefficient ( $n_{qi}\times10^2$ ) | 0.778 | 1.038 | 1.556 | 3.112 |

*Scenario 1*: Initially, four DG units are designed to share 30 kW + 6 kVar load powers proportionally as 4:3:2:1, which means that the load power served by each DG unit should be 12 kW + 2.4 kVar ($DG_1$), 9 kW + 1.8 kVar ($DG_2$), 6 kW + 1.2 kVar ($DG_3$) and 3 kW + 0.6 kVar ($DG_4$), respectively. Then, an additional 30 kW + 3 kVar load is attached at $t = 6$ s. Correspondingly, each DG will share the entire load power as 24 kW + 3.6 kVar ($DG_1$), 18 kW + 2.7 kVar ($DG_2$), 12 kW + 1.8 kVar ($DG_3$) and 6 kW + 0.9 kVar ($DG_4$).

*Scenario 2:* The load is maintained at approximately 60 kW + 9 kVar and the system settings are the same as the previous scenario. An unscheduled outage of $DG_1$ occurs at $t = 10s$. Thereafter, the load power will be shared by the remaining three DG units at a ratio of 3:2:1, which should be 30 kW + 4.5 kVar ($DG_2$), 20 kW + 3 kVar ($DG_3$), and 10 kW + 1.5 kVar ($DG_4$), respectively.

*Scenario 3*: The power sharing ratio is changed from 3:2:1 to 1:2:1 at $t = 14s$, the corresponding droop coefficients of the droop controllers and the weight coefficients of the proposed controllers are changed online to investigate the flexibility of power sharing under these two different control methods. Therefore, the updated injected power of each DG unit should be 15 kW + 2.25 kVar ($DG_2$), 30 kW + 4.5 kVar ($DG_3$), and 15 kW + 2.25 kVar ($DG_4$).

*DHC Method:* It can be seen from Fig. 4(a)-(b) that with the help of virtual impedance and proper droop coefficients, in the steady state both active and reactive power can be properly shared with the DHC method according to the preset droop coefficients. However, power fluctuations occur during the load change in Scenario 1. In the meantime, the sharing process, which is based on the primary control, causes a deviation in the frequency and amplitude of the PCC voltage, as shown in Fig. 4(c). Notice that after more than 2 s, the frequency and amplitude of the PCC voltage are recovered to their normal values, and the injected power of each DG unit

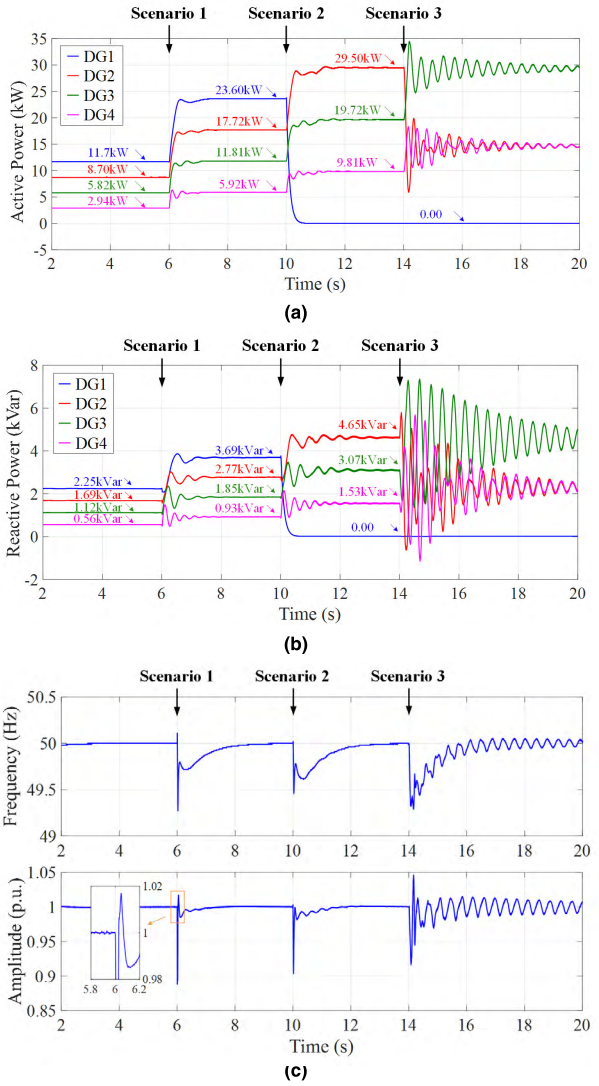


**FIGURE 4. Real-time simulation results of the DHC method: (a) Active power. (b) Reactive power. (c) Frequency and amplitude of PCC voltage.**

is gradually raised to the desired steady state value with the help of secondary coordination.

Similarly, a larger deviation in the frequency and amplitude of the PCC voltage occurs after the $DG_1$ outage in Scenario 2. Although it can be compensated by the secondary control, the relatively long transient process significantly degrades the system dynamic and affects the power supply reliability.

Furthermore, in order to fulfill the power sharing demand in Scenario 3 with a fast response speed, the droop coefficients of $DG_2$ are directly changed to the same value as $DG_4$. From Fig. 4(a) and (b) one can see that large power fluctuations occur during the droop coefficients variation. While the transient responses of the PCC voltage frequency and amplitude also have obvious cyclical oscillations, deviations still exist. It can be inferred that the overcurrent is inevitable during this transient, which may cause the quit operation of the DG units, and seriously affect the stability of the microgrid system.

*Proposed Method:* The active power can be accurately shared in the steady state, and the accuracy of the reactive power sharing is also acceptable, as shown in Fig. 5(a) and (b). Notice that the proportional power sharing is still working after the DG outage in Scenario 2. Compared with the DHC method, both the active and reactive power have faster responses during the transient, and the system can immediately arrive to the steady state in both Scenario 1 and Scenario 2.

From Fig. 5(c), it can be observed that a small frequency oscillation (0.15 Hz) occurs at the moment of load change for a very short time, which may be caused by the frequency measurement error. Afterwards, it is shown to be maintained at the rated value. It is noted that there are two undesired voltage amplitude deviations that occur at the moment of the load increase and DG outage. For the first deviation, a large load change is considered (almost the same amount as the initial load), and the deviation of the amplitude is relatively small (0.0062 p.u.), which has a minor effect on voltage regulation performance. Another small deviation is due to the condition $\sum_{i=2}^{4} m_i = 1$, which cannot be satisfied after the DG outage. According to the analysis in Section IV, it can be compensated by updating the weight coefficients. Here, we manually adjust the weight coefficient to 0.5, 0.33 and 0.17, respectively from $m_2$ to $m_4$ at $t = 11s$. It can be seen from Fig. 5(c) that the voltage amplitude is restored afterwards. In the meantime, the injected power of each DG unit is raised to the desired value, as shown in Fig. 5(a) and (b).

In Scenario 3, when the weight coefficients are updated as 0.25, 0.5 and 0.25 from $m_2$ to $m_4$, respectively, each DG unit adjusts its active and reactive power accordingly and quickly and shares the proportional power very accurately. Additionally, this process has no impact on the PCC voltage regulation, which ensures the stability of the system.

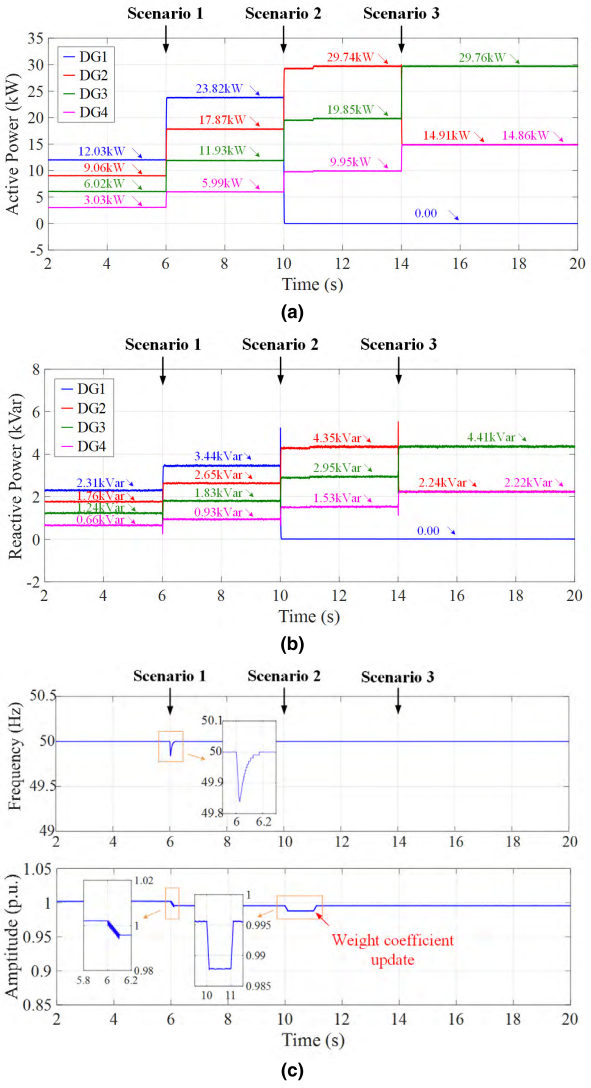


**FIGURE 5.** Real-time simulation results of the proposed method: (a) active power. (b) Reactive power. (c) Frequency and amplitude of the PCC voltage.

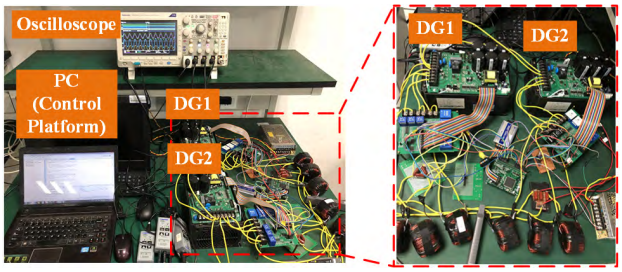


**FIGURE 6.** Experimental setup.

### B. HARDWARE EXPERIMENTAL TESTS

In this section, a microgrid prototype is built based on two parallel connected three-phase inverters and a load, as shown in Fig. 6. The experimental parameters are listed in Table 2. The practicality of the proposed controller is investigated through three cases: the load change, additional DG plug-in and flexible power sharing. For Case 1 and Case 2, the virtual impedance based droop control method is compared with

**TABLE 2. Experimental parameters.**

| | |
|---|---|
| DC source voltage | $V_{dc} = 500\,\mathrm{V}$ |
| AC phase-voltage reference | $f^* = 50\,\mathrm{Hz}$ , $V^* = 240\,\mathrm{V}$ |
| Filter parameters | $L_f = 4\,\mathrm{mH}$ , $C_f = 1\,\mathrm{uF}$ |
| Line impedances | $R_{l1} = 1.0\Omega$ , $R_{l2} = 0.5\Omega$ |
| $P$-$\omega$ droop coefficients | $n_{p1} = 4\times10^{-4}$ , $n_{p2} = 4\times10^{-4}$ |
| $Q$-$V$ droop coefficients | $n_{q1} = 2\times10^{-4}$ , $n_{q2} = 2\times10^{-4}$ |
| Preset weight coefficients | $m_1 = 0.5$ , $m_2 = 0.5$ |
| Load #1/Load #2 | $R_{load1} = 30\Omega$ , $R_{load2} = 100\Omega$ |

the proposed control strategy. The experimental results are illustrated from Fig. 7 to Fig. 9.

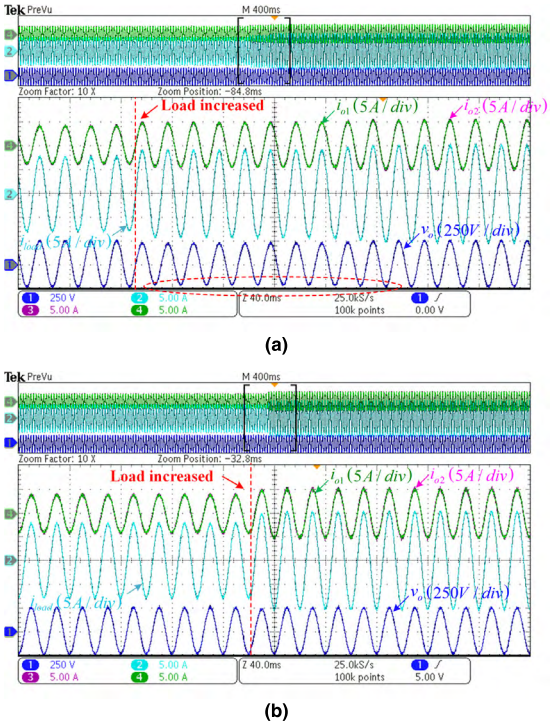


**FIGURE 7. Experimental results of Case 1. (a) Droop-based control method. (b) Proposed control method.**

*Case 1 (Response to Load Step Change):* The power sharing ratio of the two inverters is set as 1:1, and load #2 is attached to the PCC at a certain moment. Fig. 7(a) shows the transient response of the system under droop control when a load change is suddenly produced. Note that the current waveform of one inverter almost coincides with the other throughout the entire runtime. However, before the system goes to steady state, the transient process lasts for approximately 9 cycles, during which the voltage drop can be observed, the maximum deviation is close to 8% of the voltage amplitude. Compared to that, the proposed control strategy has a better transient performance as shown in Fig. 7(b), and the power sharing accuracy can also be ensured.

*Case 2 (Response to New DG Unit Plug in):* The system transient response to the DG plug-in is investigated in this case. For a droop controller, presynchronization is required for a new DG connection, which commonly requires the help of the secondary controller to acquire the PCC voltage information. Here, the power sharing ratio of the droop controllers is set as 1:1, and synchronization is achieved before one DG plugs into the system. The results are shown in Fig. 8(a). It can be seen that although the load current and PCC voltage can be maintained, the transient performance of the inverter feeding current is poor, which suffers from a fluctuation and lasts for a relatively long time. For the proposed controller, the power sharing ratio is set as 2:1, since each DG unit is controlled to track the sinusoidal references with the same frequency, phase and amplitude, and the extra presynchronization can be eliminated. As shown in Fig. 8(b), a superior transient performance and accurate power sharing can be obtained, and the PCC voltage is well-maintained during the transient.

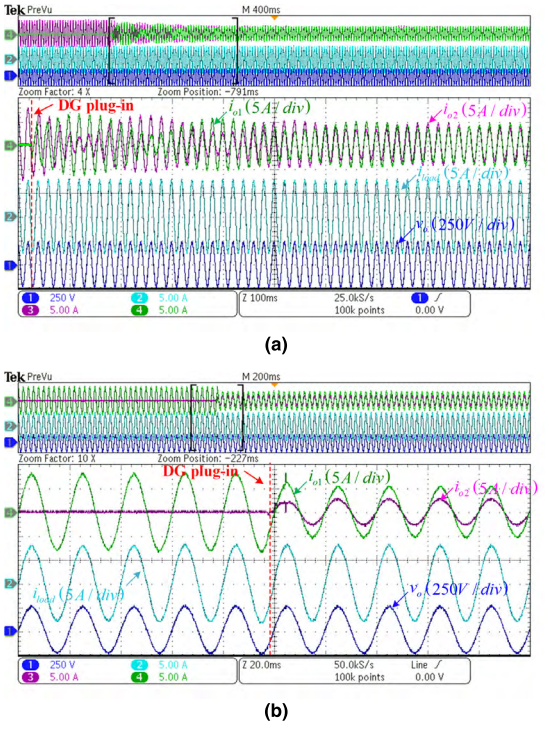


**FIGURE 8. Experimental results of Case 2. (a) Droop-based control method. (b) Proposed Control method.**

*Case 3 (Response to Weight Coefficients Adjustment):* The transient response of the proposed controller under the change of load sharing demand from 2:1 to 1:1 is tested in this case. The weight coefficient of each DG is changed from $m_1 = 0.67, m_2 = 0.33$ to $m_1 = 0.5, m_2 = 0.5$, and the results are shown in Fig. 9. It can be seen that the power sharing ratio can be accurately adjusted according to the weight coefficient in a very quick manner, while the voltage and the load current can be maintained well during this process.

Above all, the potential benefits and limitations of the proposed control method compared with the droop-based

**TABLE 3. Potential benefits and limitations of proposed method and droop based hierarchical control method.**

| | Potential Benefits | Potential Limitations |
|---|---|---|
| **Proposed Method** | ✓ Improved transient performance;<br>✓ No extra secondary control requirement;<br>✓ No trade-off between power sharing accuracy and voltage regulation quality;<br>✓ Power sharing ratio can be online adjusted; | × Relatively long distance communication is needed to acquire common bus voltage. |
| **DHC Method** | ✓ Measurements are all based on local information;<br>✓ Accurate power sharing can be realized with the integration of secondary control and virtual impedance loop. | × Relatively poor transient performance;<br>× Additional secondary control is needed to restore the voltage and frequency;<br>× Hard to design the virtual impedance when the system impedance is complex. |

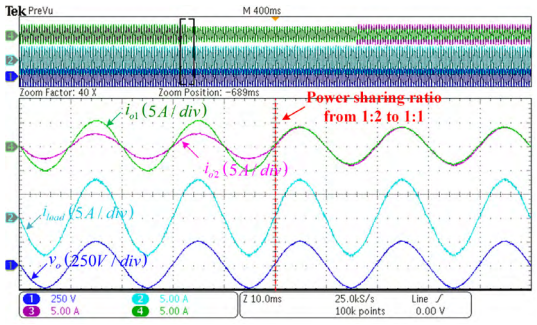


**FIGURE 9. Experimental results of Case 3 for the proposed control method.**

control method are summarized in Table 3. From the Table, it is difficult for only one control scheme to overcome all drawbacks. However, the proposed control scheme might shed some new light on the operation of grid-forming inverters to help improve the design and implementation of future islanded microgrid.

## VI. CONCLUSION

This paper presents a novel decentralized control strategy for multiple three-phase paralleled grid-forming DG units in an islanded microgrid. By using the filtered tracking error method, the proposed controller can achieve superior PCC voltage regulation and proportional load power sharing performance. Compared with the droop-based hierarchical control methods, a high transient performance can be ensured under various disturbances, i.e., large load variation, DGs fault outage and an additional DG plug-in. Moreover, flexible load power sharing among DG units can be achieved by directly adjusting the weight coefficients. Meanwhile, the voltage regulation performance will not be affected. The voltage regulation performance and the power sharing capability are analytically proven using the Lyapunov method. The effectiveness of the proposed method has been verified through a real-time simulation, as well as through hardware experiments. In the future, more advanced control algorithms for weight coefficient calculation can be integrated to achieve flexible and optimal power management of the microgrid.

## REFERENCES

[1] J. A. P. Lopes, C. L. Moreira, and A. G. Madureira, "Defining control strategies for microgrids islanded operation," *IEEE Trans. Power Syst.*, vol. 21, no. 2, pp. 916–924, May 2006.

[2] W. Guo and L. Mu, "Control principles of micro-source inverters used in microgrid," *Protection Control Modern Power Syst.*, vol. 1, no. 1, p. 5, Dec. 2016.

[3] Q.-C. Zhong, "Robust droop controller for accurate proportional load sharing among inverters operated in parallel," *IEEE Trans. Ind. Electron.*, vol. 60, no. 4, pp. 1281–1290, Apr. 2013.

[4] L. Lin, H. Ma, and Z. Bai, "An improved proportional load-sharing strategy for meshed parallel inverters system with complex impedances," *IEEE Trans. Power Electron.*, vol. 32, no. 9, pp. 7338–7351, Sep. 2017.

[5] J. W. Simpson-Porco, F. Dörfler, and F. Bullo, "Synchronization and power sharing for droop-controlled inverters in islanded microgrids," *Automatica*, vol. 49, no. 9, pp. 2603–2611, 2013.

[6] R. Majumder, B. Chaudhuri, A. Ghosh, R. Majumder, G. Ledwich, and F. Zare, "Improvement of stability and load sharing in an autonomous microgrid using supplementary droop control loop," *IEEE Trans. Power Syst.*, vol. 25, no. 2, pp. 796–808, May 2010.

[7] M. B. Delghavi and A. Yazdani, "An adaptive feedforward compensation for stability enhancement in droop-controlled inverter-based microgrids," *IEEE Trans. Power Del.*, vol. 26, no. 3, pp. 1764–1773, Jul. 2011.

[8] J. Lai, H. Zhou, X. Lu, X. Yu, and W. Hu, "Droop-based distributed cooperative control for microgrids with time-varying delays," *IEEE Trans. Smart Grid*, vol. 7, no. 4, pp. 1775–1789, Jul. 2016.

[9] D. E. Olivares *et al.*, "Trends in microgrid control," *IEEE Trans. Smart Grid*, vol. 5, no. 4, pp. 1905–1919, Jul. 2014.

[10] A. Haddadi, A. Yazdani, G. Joós, and B. Boulet, "A gain-scheduled decoupling control strategy for enhanced transient performance and stability of an islanded active distribution network," *IEEE Trans. Power Del.*, vol. 29, no. 2, pp. 560–569, Apr. 2014.

[11] I. Ziouani, D. Boukhetala, A.-M. Darcherif, B. Amghar, and I. El Abbassi, "Hierarchical control for flexible microgrid based on three-phase voltage source inverters operated in parallel," *Int. J. Elect. Power Energy Syst.*, vol. 95, pp. 188–201, Feb. 2018.

[12] L. Che, M. Shahidehpour, A. Alabdulwahab, and Y. Al-Turki, "Hierarchical coordination of a community microgrid with AC and DC microgrids," *IEEE Trans. Smart Grid*, vol. 6, no. 6, pp. 3042–3051, Nov. 2015.

[13] J. M. Guerrero, J. C. Vasquez, J. Matas, L. G. de Vicuna, and M. Castilla, "Hierarchical control of droop-controlled AC and DC microgrids—A general approach toward standardization," *IEEE Trans. Ind. Electron.*, vol. 58, no. 1, pp. 158–172, Jan. 2011.

[14] F. Dörfler, J. W. Simpson-Porco, and F. Bullo, "Breaking the hierarchy: Distributed control and economic optimality in microgrids," *IEEE Trans. Control Netw. Syst.*, vol. 3, no. 3, pp. 241–253, Sep. 2016.

[15] A. Milczarek, M. Malinowski, and J. M. Guerrero, "Reactive power management in islanded microgrid—Proportional power sharing in hierarchical droop control," *IEEE Trans. Smart Grid*, vol. 6, no. 4, pp. 1631–1638, Jul. 2015.

[16] K. Liu and F. L. Lewis, "Robust control techniques for general dynamic systems," *J. Intell. Robotic Syst.*, vol. 6, no. 1, pp. 33–49, 1992.

[17] J.-J. E. Slotine and W. Li, *Applied Nonlinear Control*, vol. 199, no. 1. Englewood Cliffs, NJ, USA: Prentice-Hall, 1991.
[18] N. Fischer, Z. Kan, R. Kamalapurkar, and W. E. Dixon, "Saturated RISE feedback control for a class of second-order nonlinear systems," *IEEE Trans. Autom. Control*, vol. 59, no. 4, pp. 1094–1099, Apr. 2014.
[19] R. Kamalapurkar, N. Fischer, S. Obuz, and W. E. Dixon, "Time-varying input and state delay compensation for uncertain nonlinear systems," *IEEE Trans. Autom. Control*, vol. 61, no. 3, pp. 834–839, Mar. 2016.
[20] J. A. Juárez-Abad, J. Linares-Flores, E. Guzmán-Ramírez, and H. Sira-Ramírez, "Generalized proportional integral tracking controller for a single-phase multilevel cascade inverter: An FPGA implementation," *IEEE Trans. Ind. Informat.*, vol. 10, no. 1, pp. 256–266, Feb. 2014.
[21] C. Qi *et al.*, "Decentralized DC voltage and power sharing control of the parallel grid converters in multi-terminal DC power integration system," *IEEE Trans. Sustain. Energy*, to be published.
[22] J. C. Vásquez, J. M. Guerrero, M. Savaghebi, J. Eloy-Garcia, and R. Teodorescu, "Modeling, analysis, and design of stationary-reference-frame droop-controlled parallel three-phase voltage source inverters," *IEEE Trans. Ind. Electron.*, vol. 60, no. 4, pp. 1271–1280, Apr. 2013.
[23] X. Wang and X. Liu. (Nov. 2016). *Modeling Tech: Power Electronics HIL Teaching Laboratory*. [Online]. Available: http://www.modeling-tech.com

**XIN HUANG** (S'16) received the M.S. degree in electrical engineering from the University of Shanghai for Science and Technology, Shanghai, China, in 2015. He is currently pursuing the Ph.D. degree with the Department of Electrical Engineering, Shanghai Jiao Tong University, China.

His current research interests include islanded micro-grid analysis and inverter control.

**KEYOU WANG** (S'05–M'09) received the B.S. and M.S. degrees in electrical engineering from Shanghai Jiao Tong University, Shanghai, China, in 2001 and 2004, respectively, and the Ph.D. degree in electrical engineering from the Missouri University of Science and Technology, Rolla, MO, USA, in 2008.

He is currently a Professor and the Vice Chair with the Department of Electrical Engineering, Shanghai Jiao Tong University. His research interests include power system dynamic and stability, renewable energy integration, and power electronic-dominated systems. He serves as an Associate Editor of the *IET Generation, Transmission and Distribution* and as an Academic Editor of the *CSEE Journal of Power and Energy Systems.*

**JIAN QIU** was born in Ningbo, China. He received the B.S. degree in automation from Northeast University, Qinhuangdao, China, in 2016. He is currently pursuing the M.S. degree in electrical engineering with Hangzhou Dianzi University, Hangzhou, China.

His current research interests include power electronic digital control, modular multilevel converters, and ac machine drives.

**LIJUN HANG** (M'09) received the B.S. and Ph.D. degrees in electrical engineering from Zhejiang University, Hangzhou, China, in 2002 and 2008, respectively. where she was a Postdoctoral Researcher, from 2008 to 2011.

From 2011 to 2013, she was a Research Assistant Professor with CURENT, University of Tennessee, Knoxville, TN, USA. She is currently a Professor with Hangzhou Dianzi University, Hangzhou. She has authored or co-authored more than 80 published technical papers. Her research interests include digital control of power electronics for grid-connected converters, converters for micro-grid, and renewable energy.

**GUOJIE LI** (M'09–SM'12) received the B.E. and M.E. degrees in electrical engineering from Tsinghua University, Beijing, China, in 1989 and 1993, respectively, and the Ph.D. degree from the School of Electrical and Electronic Engineering, Nanyang Technological University, Singapore, in 1999.

He was an Associate Professor with the Department of Electrical Engineering, Tsinghua University. He is currently a Professor with the Department of Electrical Engineering, Shanghai Jiao Tong University, Shanghai, China. His current research interests include ac/dc power system analysis and control, wind and PV power control and integration, and DAB control.

**XINGANG WANG** received the M.S. degree in electrical engineering from Shanghai Jiao Tong University, Shanghai, China, in 2009. He serves as the Departmental Associate Director of the Electric Power Research Institute, State Grid Shanghai Municipal Electric Power Company. His research interests include electric energy metering and distribution network monitoring.